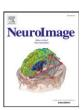
EL SEVIER

Contents lists available at ScienceDirect

NeuroImage

journal homepage: www.elsevier.com/locate/ynimg



Altered structural connectome in adolescent socially isolated mice



Cirong Liu ^{a,b,c}, Yonghui Li ^a, Timothy J. Edwards ^a, Nyoman D. Kurniawan ^d, Linda J. Richards ^{a,e}, Tianzi Jiang ^{a,b,c,f,*}

- ^a Queensland Brain Institute, The University of Queensland, Brisbane, QLD 4072, Australia
- ^b Brainnetome Center, Institute of Automation, Chinese Academy of Sciences, Beijing 100190, China
- ^c National Laboratory of Pattern Recognition, Institute of Automation, Chinese Academy of Sciences, Beijing 100190, China
- ^d The Centre for Advanced Imaging, The University of Queensland, Brisbane, QLD 4072, Australia
- ^e The School of Biomedical Sciences, The University of Queensland, Brisbane, QLD 4072, Australia
- f Key Laboratory for NeuroInformation of Ministry of Education, School of Life Science and Technology, University of Electronic Science and Technology of China, Chengdu 610054, China

ARTICLE INFO

Article history: Received 11 February 2016 Revised 11 June 2016 Accepted 18 June 2016 Available online 20 June 2016

Keywords:
Brain network
Connectome
Structural connectivity
Diffusion MRI
Orbitofrontal cortex
Social deprivation

ABSTRACT

Social experience is essential for adolescent development and plasticity of social animals. Deprivation of the experience by social isolation impairs white matter microstructures in the prefrontal cortex. However, the effect of social isolation may involve highly distributed brain networks, and therefore cannot be fully explained by a change of a single region. Here, we compared the connectomes of adolescent socially-isolated mice and normal-housed controls *via* diffusion magnetic resonance imaging. The isolated mice displayed an abnormal connectome, characterized by an increase in degree and reductions in measures such as modularity, small-worldness, and betweenness. The increase in degree was most evident in the dorsolateral orbitofrontal cortex, entorhinal cortex, and perirhinal cortex. In a connection-wise comparison, we revealed that most of the abnormal edges were inter-modular and inter-hemispheric connections of the dorsolateral orbitofrontal cortex. Further tractography-based analyses and histological examinations revealed microstructural changes in the forceps minor and lateral-cortical tracts that were associated with the dorsolateral orbitofrontal cortex. These changes of connectomes were correlated with fear memory deficits and hyper-locomotion activities induced by social isolation. Considering the key role of the orbitofrontal cortex in social behaviors, adolescent social isolation may primarily disrupt the orbitofrontal cortex and its neural pathways thereby contributing to an abnormal structural connectome.

© 2016 Elsevier Inc. All rights reserved.

1. Introduction

Social experience is important for normal brain development and plasticity of social animals, particularly during adolescence. Social isolation not only induces stress but also deprives the animal of essential experiences required for normal brain maturation and plasticity (Blakemore and Mills, 2014; Fuhrmann et al., 2015), which have been studied extensively in rodent animal models (Buwalda et al., 2011). Recent studies have begun to examine the effect of social isolation on white matter development: social isolation during the first two weeks post-weaning causes detrimental hypo-myelination in the medial prefrontal cortex (PFC) (Makinodan et al., 2012), and chronic social isolation during adolescence and young adulthood causes similar effects (Liu et al., 2012). However, the effect of social isolation may involve

highly distributed brain regions, and therefore cannot be fully explained by a change to a single brain region.

Instead of limiting analysis to particular regions or tracts, we can model the complex system as a large-scale network or connectome that fully describes the structural architecture of the brain (Sporns et al., 2005). Recent advances in diffusion magnetic resonance imaging (dMRI) and tractography have enabled the connectivity profiles of the entire brain to be mapped, and have greatly promoted the exploration of the human structural connectome (Sporns et al., 2005). These dMRI-based studies of the human connectome have deepened our understanding of normal brain development and neurodevelopmental disorders such as depression, schizophrenia, and autism (Griffa et al., 2013; Zuo et al., 2012). In contrast to the multitude of discoveries regarding the human connectome, only one dMRI-based study investigated the maturation of the mouse structural connectome, which quantified the brain changes in connectivity during development and revealed a nonlinear relationship between network measures and age (Ingalhalikar et al., 2015).

In this study, we investigated how social isolation during adolescent development affected brain's structural connectome. We acquired high-

^{*} Corresponding author at: Queensland Brain Institute, The University of Queensland, Brisbane, QLD 4072, Australia; Brainnetome Center, National Laboratory of Pattern Recognition, Institute of Automation, Chinese Academy of Sciences, Beijing 100190, China. *E-mail address:* jiangtz@nlpr.ia.ac.cn (T. Jiang).

resolution *ex-vivo* dMRI from normal-housed controls and socially isolated C57BL/6 mice. Based on dMRI, we created an atlas and performed probabilistic tractography to construct the structural connectome. The structural connectomes of the two groups were then compared *via* graph-theory approaches (network-wise comparisons) (Rubinov and Sporns, 2010) and network based statistics (connection-wise comparisons) (Zalesky et al., 2010). We then investigated the association between properties of the structural connectome and behavioral phenotypes. Finally, we performed tractography-based analyses and histology to examine the white matter tracts that may contribute to the abnormal structural connectome. These comprehensive analyses allow us to fully describe the structural connectome in socially isolated mice and facilitate the understanding of social experience in adolescent brain development and plasticity.

2. Materials and methods

2.1. Animals

Thirty-two C57BL/6 mice (18 males and 14 females) were divided into two groups: control (C; 10 males and 7 females) and socially isolated (I; 8 males and 7 females). Mice in the control group were group-housed in standard transparent plastic cages (3 or 4 mice per cage), while mice in the isolated group were housed separately (1 mouse per cage) from postnatal day 35 (P35) for 4 weeks. Behavioral tests were performed from P57 to P61, including an open-field test (1 day), a Y-maze spontaneous alternation test (1 day) and a fear conditioning test (3 days). All mice were housed and handled in accordance with the Queensland Animal Care and Protection Act 2001 and the current NHMRC Australian Code of Practice for the Care and Use of Animals for Scientific Purposes (UQ ethics approval QBI/262/12/RSA).

2.2. Behavioral tests

The open-field test was used to assess novel environment-induced locomotor activity (Walsh and Cummins, 1976). Mice were placed in a transparent cage with the light intensity adjusted to 85 lx (Activity Monitor system, MED Associates, Inc., St. Albans, VT, USA), and locomotion was measured for 2 h using digital counters with infrared sensors. One male socially isolated mouse and 6 female mice (3 controls and 3 socially isolated mice) were excluded from the open field test due the failures of equipment.

The Y-maze spontaneous alternation test was used to assess spatial working memory based on the animal's innate disposition to alternate between arms of the maze (Dember and Fowler, 1958). The Y-maze was composed of three connected transparent acrylic arms (L40 cm \times W10 cm \times H22 cm) separated by 120°, and visual cues including chairs, rubbish bins, boxes and curtains $\it etc.$ were placed in the room to assist the mice in distinguishing different directions. A camera was positioned above the maze for video recording and the light intensity was adjusted to 85 lx. The test lasted for 8 min and the sequence of arm entries was recorded. The percentage of alternation was the number of trials containing consecutive entries into all three arms divided by the number of all alternations.

The fear conditioning test was used to assess fear memory. Fear conditioning is a form of classical conditioning involving the repeated pairing of a non-threatening stimulus (conditioned stimulus) with an aversive stimulus (unconditioned stimulus) (Maren, 2001). The fear conditioning protocol we employed was similar to a previous study (Pattwell et al., 2011), including one conditioning day followed by two test days. On the conditioning day, mice were placed in a mouse test chamber (Coulbourn Instruments, Whitehall, PA, USA) inside a sound-attenuated box with white walls and an electrified floor grid. After a 2-minute acclimation, mice were conditioned with three pairs of conditioning and un-conditioning stimuli (CS–US) that consisted of a 30-second tone (5 kHz, 70 dB) coincident with a 1-second, 0.7-mA foot

shock delivered through the electrified floor grid. Individual pairings were separated by a 30-second inter-trial interval. After the final CS–US pairing, mice remained in the chamber for 1 min before being returned to their home cages. Twenty-four hours later, mice were assessed for contextual fear memory, which was carried out in the same chamber as the conditioning day. Freezing behavior was scored during the 5.5 min in the chamber used for the contextual fear conditioning. Forty-eight hours later, mice were assessed for cued fear memory in a new chamber with black walls and a smooth green plastic floor. After a 2-minute acclimation, mice were presented with three 30-second tones (5 kHz, 70 dB) separated by an inter-trial interval of 30 s. After the last tone, mice stayed in the chamber for 1 min before being returned to their home cages. Freezing behavior was scored during the 30-second tone presentations for the tone (cued) fear conditioning.

2.3. Diffusion MRI data acquisition

After behavioral tests, mice were perfused and prepared for MRI scanning. The animals were anesthetized with lethabarb (VIRBAC PTY, Australia) and perfused with 0.1 M phosphate buffered solution (PBS; BioWhittaker, USA) followed by 4% paraformaldehyde (pH 7.4; Sigmaaldrich, USA) in PBS, and further post-fixed for 24 h. The brain samples were then stored in 0.1 M PBS with 0.02% sodium azide (Sigma-aldrich, USA). Before MRI scanning, the brains were immersed in 0.1 M PBS with 0.2% gadopentetate dimeglumine (Magnevist, Bayer, Leverkusen, Germany) for four days to enhance MRI contrast. Diffusion-weighted magnetic resonance images were acquired using a 16.4T vertical bore, small animal MRI system (Bruker Biospin, Rheinstetten, Germany; ParaVision v5.0) equipped with Micro2.5 imaging gradient and a 15 mm linear surface acoustic wave coil (M2M, Brisbane, Australia). Three-dimensional diffusion-weighted spin-echo sequences were acquired using the following parameters: repetition time = 400 ms, echo time = 20 ms, δ/Δ = 2.5/12 ms, field of view = 18.99 × 11.16 × 8 mm, matrix = $190 \times 112 \times 80$, bandwidth = 50 kHz, 30 direction diffusionencoding with b-value = 5000 s/mm², 2 b0 images acquired without diffusion-weighting and 0.1 mm isotropic resolution. Acquisition time for one brain was 15 h with 1.5 partial Fourier encoding acceleration in the phase dimensions.

2.4. Construction of structural connectomes

Nodes and edges are two key components of structural connectomes. Below, we first explain how the atlas was constructed to define the nodes (Fig. 1A–B), and then describe how the edges between each pair of nodes were computed *via* probabilistic tractography (Fig. 1C–D).

2.4.1. Atlas construction: defining nodes

The first step of network construction was to define regions of interest (ROIs) as nodes (Fig. 1A-B). Two ex-vivo MRI-based atlases of adult C57BL/6 mouse were utilized to create these ROIs: one from the Centre for Advanced Imaging at The University of Queensland (CAI atlas) and the other from the Mori lab of Johns Hopkins University (JHU atlas). The CAI atlas was created using the same 16.4T small animal MRI system as the current study (Ullmann et al., 2013), which provided fine-grained parcellations of the mouse neocortex but lacked the subcortical structures. The JHU atlas provided subcortical structures but the cortex was not parcellated (Chuang et al., 2011). The JHU template (T2 image) was first spatially transformed (affine transformation followed by nonlinear deformation) to the CAI template (T2 image) by Advanced Normalization Tools (ANTs, http://stnava.github.io/ANTs/), and then ROIs from the two atlases were merged to form a combined atlas with 78 ROIs (39 on each hemisphere, see Supplementary Table S1) that covered all major cortical and subcortical brain regions. The combined atlas was mapped (affine transfromation followed by nonlinear deformation) to

Download English Version:

https://daneshyari.com/en/article/6023441

Download Persian Version:

https://daneshyari.com/article/6023441

<u>Daneshyari.com</u>